Eur. Phys. J. Plus (2017) **132**: 176
DOI 10.1140/epjp/i2017-11312-5

THE EUROPEAN PHYSICAL JOURNAL PLUS

Regular Article

Alternate current conductivity in BSb films prepared by PLD technique: Electron transport processes in low-temperature range (10–275 K)

Shirsendu Das[1], Ritamay Bhunia[1], Shamima Hussain[1,2], Radhaballabh Bhar[1], and Arun Kumar Pal[1,a]

[1] Department of Instrumentation Science, Jadavpur University, Kolkata - 700032, India
[2] UGC-DAE CSR, Kalpakkam Node, Kokilamedu - 603104, India

Received: 8 September 2016 / Revised: 1 December 2016
Published online: 17 April 2017 –

Abstract. This study is focused on the measurement of alternate current (a.c.) electrical conductivity of BSb films, deposited on fluorine-doped tin oxide (FTO)–coated glass substrates at 673 K by the pulsed laser deposition (PLD) technique. The frequency-dependent a.c. conductivity is measured as a function of temperature (10–275 K) and frequency (100 Hz–100 kHz). The transport processes governing the electrical conduction processes in this material are analyzed critically. It is observed from FESEM micrograph that the film is composed of small discrete grain with sizes varying in the range 6–12 nm. It is interesting to notice from $\ln \sigma_{ac}$ *versus* 1000/T plot that there are three distinct zones: i) Semiconductor zone at high temperature from 275 to 150 K, ii) Insulator zone at low temperature from 70 to 10 K and iii) an abrupt change of the $\ln \sigma_{ac}$ *versus* 1000/T plot at ~ 75 indicating MIS transition occurring in this BSb film. We found that the activation energy for the BSb films in the lower-temperature range was quite low ~ 6 to 41 neV, while that in the higher-temperature range was 20 to 50 meV.

1 Introduction

The binary compound BSb has emerged as an important material in current device technology. A number of theoretical works pertaining to band structure calculation [1,2] indicated its possible use in hot-carrier solar cells (HCSC) [3]. Cell structures associated with the HCSC require tuning of phononic band gap of this material. This material in nanocrystalline form also forbids thermalization due to the localization of the density of states in the extended states. This would permit the extraction of hot electrons while still in the extended states for their fruitful utilization in energy conversion in tandem cells [4]. Despite the theoretical advancement in understanding the material properties of this material, reports on successful synthesis of this material in thin-film form are not many due to some inherent difficulties. The difficulties involved in the synthesis, as discussed in details in a previous publication [5], deterred the progress of evolving a viable technique to synthesize the above material. Only recently, Das *et al.* [5] reported a successful attempt to deposit BSb films with assured composition by the PLD technique. The above success has made it more important to study the electron transport processes controlling the electron conduction behavior in these films to accelerate their use in hot-carrier solar cells.

To the best of our knowledge, there are only two reports on the measurement of d.c. electrical conductivity of BSb films [6,7]. Kumashiro *et al.* [6] reported the measurement of electrical and thermoelectric properties on $B_{12}Sb_2$ films synthesized by molecular flow region PVD method. The electrical conductivity of the films was measured by a two-probe method at temperatures between room temperature and 600 °C. The films displayed high mobility of $\sim 100\,cm^2$/V-s and high thermoelectric figures of merit of $\sim 10^{-4}$/K. Recently, Dalui *et al.* [7] reported the variation of d.c. electrical conductivity with temperature of BSb films (210–360 K) deposited by the co-evaporation method. They observed that the electron transport process in their films was governed by Mott's hopping although the values of the exponent "p" which determines the nature of the transition, varied between 1.01 and 1.3.

In this report, we present a detailed study on the variation of a.c. conductivity (σ_{AC}) measured as a function of frequency (100 Hz to 100 kHz) in the temperature range from 10 K to 275 K. Possible electron transport processes

[a] e-mail: msakp2002@yahoo.co.in (corresponding author)

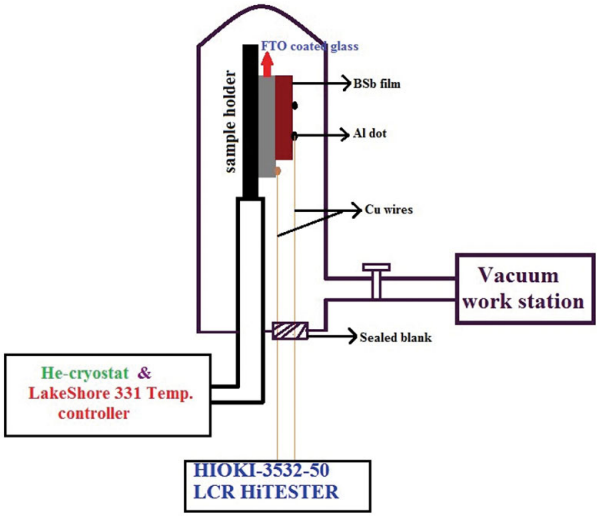

Fig. 1. Schematic diagram of a full a.c. conductivity measurement set-up.

operative in this film that would describe the observed variation of electrical conductivity in the temperature range from 10 K to 275 K faithfully are described here. To the best of our knowledge, this would be the first kind of report on a.c. conductivity measurement for the above material of device interest.

2 Experimental details

Boron antimonide films were deposited by using a conventional PLD configuration as described in ref. [5]. In short, a Nd:YAG laser (wavelength (λ) = 355 nm, duration of pulse t = 10 ns, pulse frequency = 10 Hz) was utilized to ablate the target to deposit films onto glass substrates kept at an optimal substrate temperature of 673 K. A glass lens was used to focus such that the laser beam falls on the target at an angle of 45° with respect to the normal. The laser fluence was $\sim 8\,\mathrm{J/cm^2}$ measured at the entrance focusing lens. Thus the actual fluence at the target surface would be less than the above. A detailed discussion on fluence in laser ablation technique related to tungsten and boron and their composite was discussed by Moscicki [8]. As the melting point of boron is too high ($\sim 2000\,^\circ$C) so required fluence was too high [8]. The target was rotated at ~ 10 rpm so that fast drilling could be avoided. The target and the substrate distance were maintained at ~ 4.5 cm. The base pressure of the chamber during deposition was $\sim 5 \times 10^{-6}$ Torr. All the films were deposited for 15 minutes using 9000 laser pulses. The films were deposited onto Fluorine-doped tin oxide (FTO)–coated glass substrates. The film thickness was ~ 500 nm with an area of 10 mm × 10 mm. Surface topography of the films was recorded by FESEM (Carl Zeiss AURIGA system). The films were quite uniform as has been depicted by the detailed topography studies carried out by FESEM.

It is known that the critical factor in measuring electrical conductivity of the thin films is to make proper electrode contacts to the films. Appropriate electrical contacts were obtained by depositing aluminium dots by thermal evaporation at a system pressure better than 10^{-6} Torr on the BSb film using appropriate stainless-steel mask. Contacts were obtained from the FTO film and top aluminiun dots for a.c. measurement. a.c. measurements were carried out using a HIOKI-3532-50 impedance analyzer using a.c. voltage 3 mV. Measurements were carried out using a number of aluminium dots on the BSb film and it was found that the results were well within ±1%. This also indicates the uniformity of the BSb films deposited here. The sample was mounted on the cold finger of a closed-cycle helium cryostat (fig. 1). The Cu wires were connected to the Al dot and FTO-coated glass with the help of silver paste.

3 Results and discussion

3.1 Microstructural studies

High magnification FESEM micrograph of BSb film, deposited on FTO-coated glass substrates at 673 K, is shown in fig. 2. Top left-hand inset of this figure shows the corresponding histogram and the right-hand side inset shows the FESEM picture of the same BSb film at lower magnification. It could be observed from fig. 2 that the film is composed of small discrete grain with sizes varying in the range 6–12 nm. This value matched well with that (~ 10 nm) computed from XRD measurements (not shown here) using Scherrer formula. The right-hand inset of fig. 2 indicates that the films are quite uniform and compact.

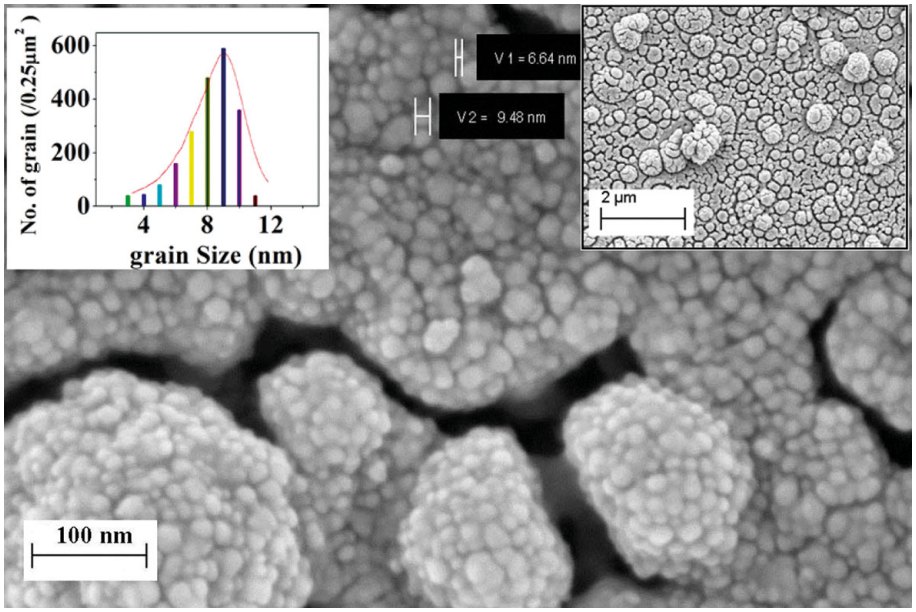

Fig. 2. High-Magnification FESEM picture of a representative film of BSb (top left inset shows the histogram and the right inset shows the FESEM picture of the same BSb film at lower magnification).

3.2 Electrical measurement: a.c. conductivity

In disordered materials, the measurement of a.c. conductivity provides information on the electronic structure of the material. Disorder in the atomic structure is associated with the creation of localized states. The oscillations induced in the polarization charges due to the presence of time-varying electric field makes a.c. measurement a useful tool for studying the electron transport processes in the hopping regime.

The variation of a.c. conductivity of the BSb films prepared as above was measured in the frequency range 100 Hz to 100 kHz (fig. 3(a)). Temperature during a.c. measurements was varied between 10 K and 275 K. The variation of the a.c. conductivity (σ_{AC}) with frequency (ω) is expressed as [9]

$$\sigma_{AC} = A\omega^{\delta}, \tag{1}$$

where, ω is the angular frequency, A is a constant and the exponent δ is a temperature-dependent quantity. The above variation of conductivity with frequency has generally been ascribed to relaxation induced by motion of charge carriers performing hopping between equilibrium sites [10–17]. Various ionically and electronically (polaronic) conductive disordered materials generally exhibit specific features associated with the electron transport processes controlling the transport processes in such materials through a log-log plot of the real part of the conductivity *versus* frequency. At low frequencies, conductivity is frequency-independent and would reflect DC conductivity. With increasing frequencies, the conductivity should start to increase in a power law fashion and are analyzed using Jonscher equation (eq. (1)).It may be observed here that there are two distinct temperature domains of σ_{AC} dependence with frequency: 175 K to 275 K (fig. 3(b)) and 10 K to 150 K (fig. 3(c)). Experimental conductive spectra (fig. 4(a)) exhibit a maximum (especially in the higher temperature region) and tend to decrease at lower temperatures. The decrease in conductivity is a typical semiconductor behaviour. The above features indicate that the exponent δ should not only be temperature-independent but also be frequency-dependent. Temperature independence of δ has generally been predicted. δ should be less than unity in the audio frequency range. On the other hand, δ may also be frequency-dependent. It should decrease as the frequency is increased.

Usually, there are three effects that contribute to the a.c. conductivity:

i) the electrode effects are active at low frequency;

ii) the DC plateau is observed at intermediate frequencies;

iii) the defect processes at higher temperature [18,19].

It may be observed that the a.c. conductivity increased with frequency, reached a peak value before decreasing with frequency. This variation is very prominent above 150 K (fig. 3(a)). The change in the slope in the conductivity spectrum this region indicates hopping frequency (ω_p) region. The peaks shift could be observed with frequency exhibited by

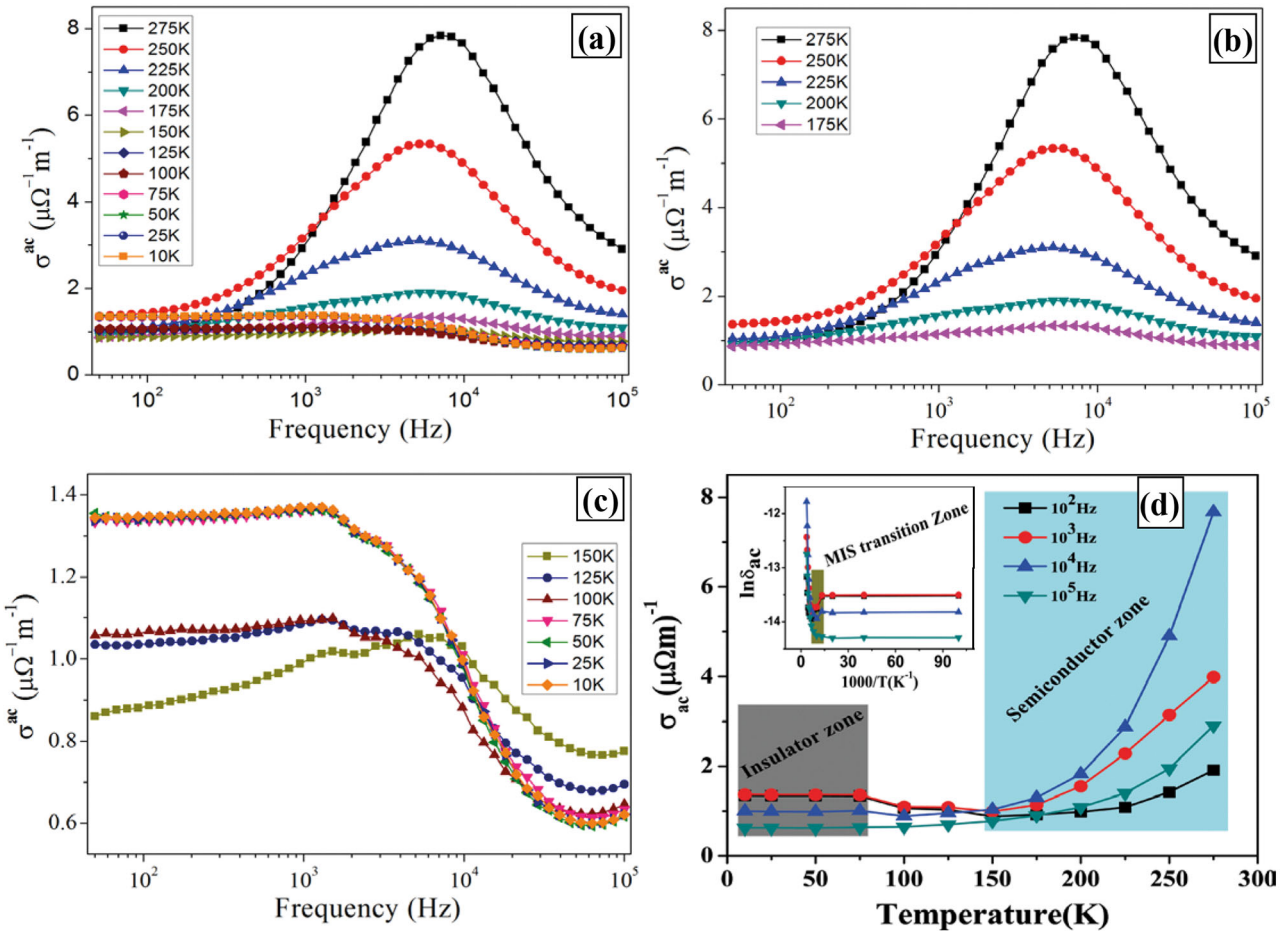

Fig. 3. (a) Variation of σ_{AC} with frequency measured at different temperatures (10–275 K), (b) variation of σ_{AC} with frequency measured at different temperatures (175–275 K), (c) variation of σ_{AC} with frequency measured at different temperatures (10–150 K) and (d) Variation of σ_{AC} with temperatures at four different frequencies of 10^2 Hz, 10^3 Hz, 10^4 Hz and 10^5 Hz (Inset shows the variation of ln(σ_{AC}) with 1000/T for a representative BSb films).

a well-defined maximum. This reflects a characteristic relaxation rate that could be associated with the above shift which would display asymmetric frequency dependence. This type of conductivity reflects its complex dependence on angular frequency (ω), dielectric loss (ε'') and permittivity of free space (ε_0). It is known that polarization lags with a.c. field culminating in dielectric loss in a.c. conductivity measurement. Dielectric dispersion would occur due to different kinds of polarizations in different frequency ranges and dependence of these quantities on conductivity would decrease with frequency in the domain when the dielectric loss would decrease with frequency.

The conductivity became temperature-independent gradually with progressive increase in frequency. Figure 3(d) shows the variation of the measured σ_{AC} values with temperature in different frequency zones and the inset of fig. 3(d) shows $\ln \sigma_{AC}$ *vs.* 1000/T plot of the measured σ_{AC} values at different frequencies. It may be seen that σ_{AC} is almost temperature-independent from $\sim$ 10 K to $\sim$ 75 K (fig. 3(d)). MIS transition zone ($\sim$ 75 K) is indicated in the inset of fig. 3(d). Between 75 K and 125 K, a.c. conductivity decreased slightly with temperature indicating metallic behaviour and beyond that temperature a.c. conductivity increased sharply with the increase of temperature indicating normal semiconducting behaviour (fig. 3(d)). The electrical conduction in the material will be governed by a thermally activated process. This type of variation of conductivity with frequency has been observed as a typical one for many different materials [20–22]. In such a case, the application of a power law equation to the entire range of frequency may become questionable and analysis of exponent δ by simply using the power law as such might not be meaningful. For such systems, concept of complex variation of the exponent (δ) with temperature and frequency was introduced in form of eq. (2) shown in the next paragraph.

Let us now examine the nature of δ which may be computed from plots of $\ln \sigma_{AC}$ *versus* $\ln(\omega)$ as shown in fig. 4(a). It was observed that the dependence of the exponent δ on the frequency is much more complex (fig. 4(b) and (c)) than what has been indicated above. The exponent (δ) shows a very sharp increase from 0.2 to 0.6 with increase in frequency up to $\sim 10^3$ Hz when measured in the temperature range from 150 K to 275 K (fig. 4(b)). Above 10^3 Hz, δ

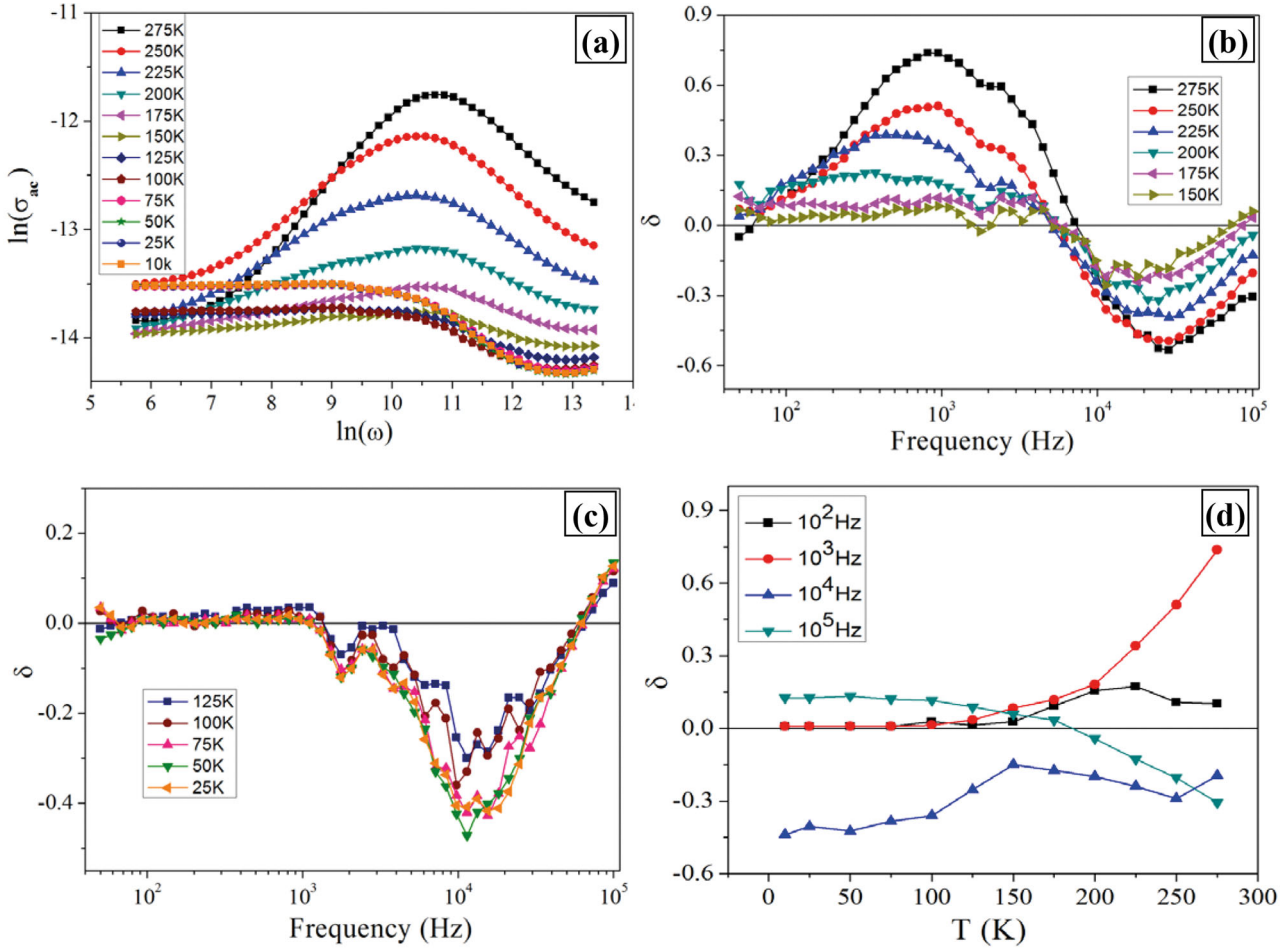

Fig. 4. (a) Plot of $\ln(\sigma_{AC})$ with $\ln(\omega)$ measured at different temperatures (10–275 K). Variation of δ with frequency measured at: (b) temperatures (150–275 K) and (c) temperatures (10–125 K), (d) variation of δ with temperature measured at four different frequencies.

started to decrease sharply with increasing frequency reaching negative values and tended to increase again showing a minimum at a frequency $\sim 2 \times 10^4$ Hz. At lower temperature of measurements (25 K to 125 K), the value of δ is extremely small and nearly invariant up to a frequency $\sim 10^3$ Hz (fig. 4(c)). Above $\sim 10^3$ Hz, δ started to decrease sharply with increasing frequency reaching negative values and tended to increase again before showing a minimum at a frequency $\sim 10^4$ Hz. The complex variation of the exponent (δ) with temperature at four frequencies is shown in fig. 4(d).

With such a complex variation of the exponent (δ) over frequency and temperature range, the a.c. conductivity may be expressed as

$$\sigma_{AC}(\omega, T) = \sigma_o + \Sigma A \omega^{\delta}, \tag{2}$$

where σ_o is the d.c. conductivity and δ corresponds to the exponent applicable to the respective hopping processes describing the electron transport processes.

Funke [23] explained that the value of δ might have a physical meaning when $\delta \leq 1$. In such a situation, the hopping motion would involve a sudden hopping in translational motion. Localized hopping of the species with a small hopping without leaving the neighborhood would be indicated by $\delta > 1$. Hopping frequency (ω_p) of the polarons is the frequency at which the slope changes. It is temperature-dependent. The origin of the frequency-dependent conductivity [24] would originate from the relaxation phenomenon arising due to mobile charge carriers. It was also reported [25] that for small polaron hopping conduction, the value of δ would increase with temperature. δ was seen to decrease with temperature for large polaron hopping conduction. Due to the limited scope, we refrained ourselves to make further comments on the observed complex dependence of δ with frequency and temperature (fig. 4(d)).

Temperature dependence of a.c. conductivity (σ_{AC}) as shown in fig. 3(d) could be revisited separately for the two distinct temperature zones of relevance as indicated in fig. 5. The above two distinct temperature zones: i) high-temperature zone form 275 to 150 K (fig. 5(a)) and ii) low-temperature zone from 75 to 10 K (fig. 5(b)) have been

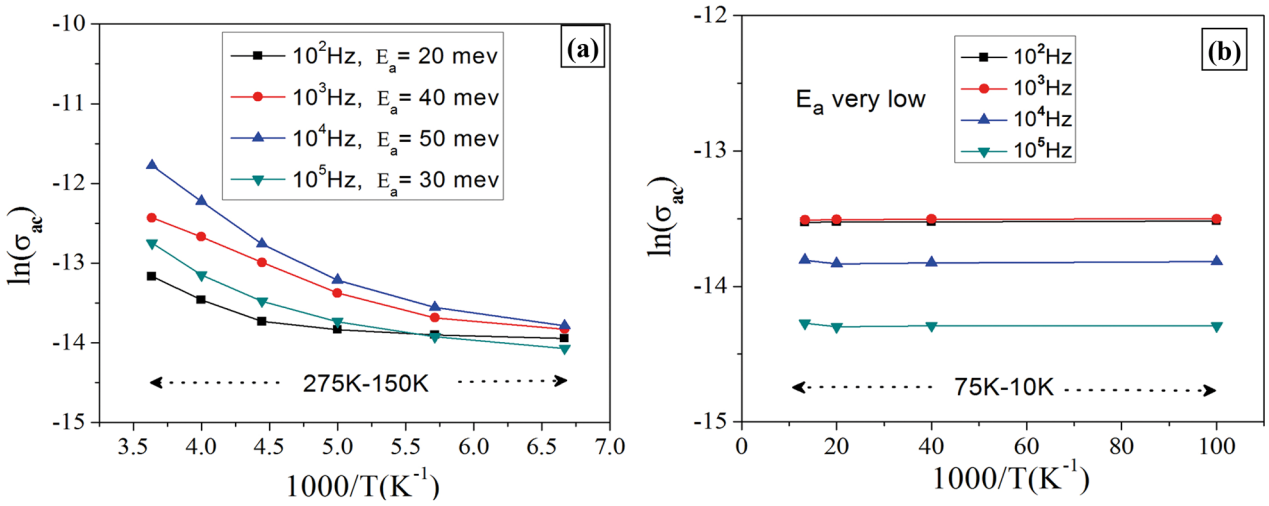

Fig. 5. (a) Plot of $\ln(\sigma_{\mathrm{AC}})$ *versus* 1000/T for the above film in the higher-temperature zone (150–275 K). (b) Plot of $\ln(\sigma_{\mathrm{AC}})$ *versus* 1000/T for the same film in the lower-temperature zone (10–75 K).

shown in expanded form to facilitate the application of hopping conduction processes in this system. Under certain conditions the Coulomb gap would exist in the low-energy electron excitation spectrum in the insulator state of a disordered system as a result of the electron-electron interaction. Hopping in the Coulomb gap would become more effective in describing the low-temperature electron transport properties. Collapsing of Coulomb gap as the critical point for the transition is reached as indicated by Pollak [26] and Zabordskii *et al.* [27,28]. It may be observed that the variation of electrical conductivity in the temperature range 75–10 K is very nearly identical for all the four frequencies (fig. 5(b)). The activation energy for the BSb films in the lower-temperature range, as obtained from the $\ln(\sigma)$ *vs.* 1000/T plots (fig. 5(b)) was quite low ($\sim$ 6 to 41 neV) while that in the higher-temperature range was 20 to 50 meV (fig. 5(a)). The values of activation energies so obtained are quite low signifying the fact that the electron transport processes would be governed by tunneling in this disordered system. At relatively lower temperatures, thermally activated hopping between localized states near the Fermi level describes the electron transport in these films. The electrons would prefer to jump longer and longer distances in order to find states closer in energy in this variable range hopping (VRH) regime in the low-temperature domain 10 K–100 K. The product of the density of states and probability distribution function is known to indicate the number of occupied states per unit volume at a given energy for a system in thermal equilibrium. This would mean that the transport will be governed by hopping within the states in the Coulomb gap. The variable range hopping (VRH) process [29] would favour an electron to jump from one localized state to another where there exists an overlap of the wave functions. The difference in the eigen energies is compensated by the absorption or emission of phonons.

The value of the index δ, particularly at lower temperature and higher frequency, may be explained on the basis of the model of Elliot [30] according to which the a.c. conductance may be expressed as

$$\sigma(\omega) = \frac{\pi^2 g_o^2 \varepsilon_o \varepsilon_{\mathrm{r}}}{24} \left[\frac{8e^2}{\varepsilon_o \varepsilon_r E_g}\right]^6 \frac{\omega^\delta}{\tau_o^\beta}, \tag{3}$$

where g_o is the density of localized states, ϵ_o is the free space permittivity, ϵ_{r} is the dielectric constant of the material, τ_o is the effective relaxation time, e is the electronic charge and β is related to δ through the following equation:

$$\delta = 1 - \beta = 1 - (6kT/E_g), \tag{4}$$

where E_g is the optical band gap. It is customary to determine the values of δ from eq. (4) by utilizing the band gap values obtained from optical studies. With these δ values and corresponding frequencies (ω) satisfying eq. (2), one generally evaluates the density of localized states (g_o) from eq. (3) for the composite films using bulk values of τ_o, ϵ_o and ϵ_{r}. But in these BSb films, dependence of δ with frequency is quite complex and as such computing g_o as indicated above would be questionable. In this study, we computed the values of g_o by utilizing δ values obtained from the experimental frequency-dependent σ_{AC} values (as shown in fig. 4(b) and (c)) for frequency values of interest. The g_o values computed as above are shown in fig. 6. It could be observed that g_o values have a Gaussian nature with frequency showing a peak near 10^3 Hz. The intensity of the peak is dependent on the temperature zone of measurement (figs. 6(a)–(d)). All the high temperature zone g_o values showed a peak value $\sim 5\times10^{27}$ m^{-3} (fig. 6(b)) with diminishing intensity peaks while the low temperature zone g_o values indicated a peak g_o value at $\sim 5 \times 10^{20}$ m^{-3} (fig. 6(d)). It is interesting to note that g_o values computed for the MIS transition region do not show any such peak (fig. 6(c)).

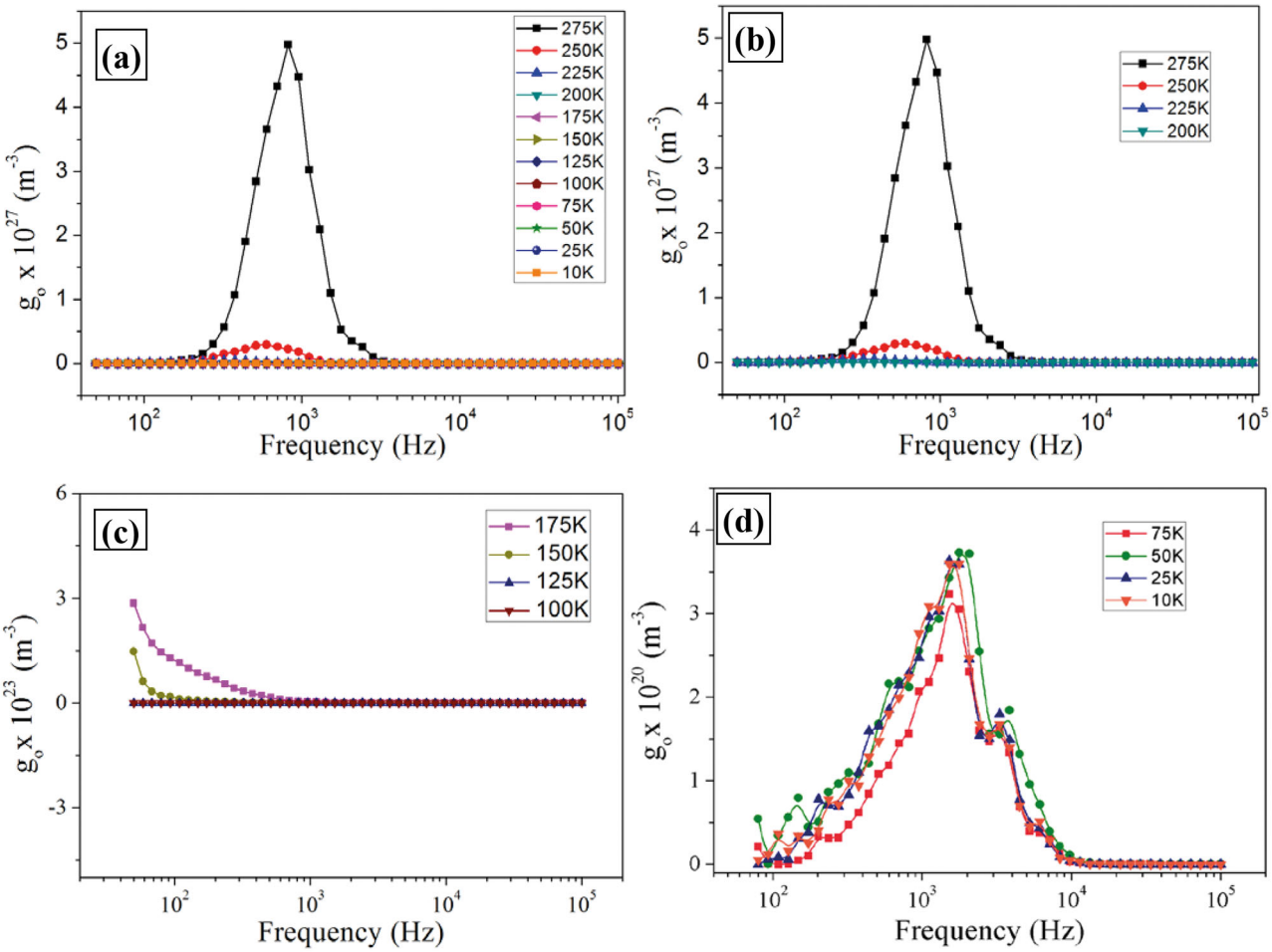

Fig. 6. (a) Plot of g_o values *versus* frequency measured at different temperatures (10–275 K). (b) Plot of g_o values *versus* frequency measured in the high-temperature range (200–275 K). (c) Plot of g_o values *versus* frequency measured at temperatures near the MIS transition region (100–175 K). (d) Plot of g_o values *versus* frequency measured in the low temperature range (10–75 K).

g_o values are very low and nearly invariant in the frequency range of 2×10^2 to 10^5 Hz. This would reflect Mott metallic minimum. It is known that at $E \sim \Delta/2$, the density of states would become equal to Mott's density of states (g_o). Considering parabolic variation of $g(E)$ within Coulomb gap (Δ), and the increasing values of density of localized states (g_o) would correspond to higher values of Coulomb gap (Δ).The activation energies (E_a) in the composite films measured at sufficiently low temperature may be identified with the value of Δ. This is quite natural since in the a.c. measurement (at higher frequency), conduction through localized states becomes most effective. It may be observed that the activation energies measured from the high frequency data tally quite well with the values of the Coulomb gap in all the films. This observation reconfirms the existence of a Coulomb gap in these composite nanocrystalline films.

4 Conclusions

a.c. conductivity measurements were carried out in the temperature range 10–275 K. It was observed that the dependence of the exponent δ on the frequency is much more complex than those reported. The exponent (δ) increased sharply from 0.2 to 0.6 with increase in frequency up to $\sim 10^3$ Hz when measured in the temperature range from 150 K to 275 K, after which δ started to decrease sharply with increasing frequency reaching negative values and tended to increase again showing a minimum at a frequency $\sim 2\times10^4$ Hz. At lower temperature of measurements (25 K to 125 K), the value of δ is extremely small and nearly invariant up to a frequency $\sim 10^3$ Hz after which δ started to decrease sharply with increasing frequency reaching negative values and tended to increase again before showing a minimum at a frequency $\sim 10^4$. Density of localized states (g_o) was computed and reported here. Metal-insulator-semiconductor transition occurring at $\sim$ 75 K was observed in this system.

The authors wish to thank the UGC-DAE CSR and Board of Research in Nuclear Sciences (BRNS) Government of India for the financial assistance for executing this programme. Fellowships awarded to S. Das and R. Bhunia by the Board of Research in Nuclear Sciences (BRNS), Government of India and the Department of Science and Technology, Government of India, respectively are acknowledged with thanks.

References

1. M. Ferhaty, B. Bouhafsz, A. Zaouiz, H. Aourag, J. Phys.: Condens. Matter **10**, 7995 (1998).
2. A. Zaoui, F.E.H. Hassan, J. Phys.:Condens. Matter. **13**, 253 (2001).
3. Y. Yao, D. König, M. Green, Sol. Energy Mater. Sol. Cells **111**, 123 (2013).
4. D. König, K. Casalenuovo, Y. Takeda, G. Conibeer, J.F. Guillemoles, R. Patterson, L.M. Huang, M.A. Green, Physica E **42**, 2862 (2010).
5. S. Das, R. Bhunia, S. Hussain, R. Bhar, B.R. Chakraborty, A.K. Pal, Appl. Surf. Sci. **353**, 439 (2015).
6. Y. Kumashiro, K. Nakamura, K. Sato, M. Ohtsuka, Y. Ohishi, M. Nakano, Y. Doi, J. Solid State Chem. **177**, 533 (2004).
7. S. Dalui, S.N. Das, S. Hussain, D. Paramanik, S. Verma, A.K. Pal, J. Cryst. Growth **305**, 149 (2007).
8. T. Moscicki, Int. J. Opt. **2016**, 5438721 (2016).
9. N.F. Mott, E.A. Davis, *Electronic Processes in Non-Crystalline Materials* (Clarendon Press, Oxford, 1979).
10. T.B. Schroder, J.C. Dyre, Phys. Rev. Lett. **101**, 025901 (2008).
11. C. Godet, J.P. Kleider, A.S. Gudovskikh, Diam. Relat. Mater. **16**, 1799 (2007).
12. J. Han, M. Shen, W. Cao, A. Senos, P.Q. Mantos, Appl. Phys. Lett. **82**, 67 (2003).
13. A.G. Hunt, Philos. Mag. B **81**, 875 (2001).
14. S. Abboudy, K. Alfaramawi, L. Abulnasr, Mod. Phys. Lett. B **28**, 1450002 (2014).
15. S.R. Elliott, Adv. Phys. **36**, 135 (1987).
16. H. Böttger, V.V. Bryksin, *Hopping Conduction in Solids* (VCH Publishers, Berlin, 1985).
17. A.L. Efros, Philos. Mag. B **43**, 829 (1981).
18. A.R. James, C.H. Prakash, G. Prasad, J. Phys. D: Appl. Phys. **39**, 1635 (2006).
19. A. Shukla, R.N.P. Choudhary, A.K. Thakur, J. Phys. Chem. Solids **70**, 1401 (2009).
20. S.K. Barik, R.N.P. Choudhary, A.K. Singh, Adv. Mater. Lett. **2**, 419 (2011).
21. M. Krichen, M. Megdiche, M. Gargouri, K. Guidara, Indian J. Phys. **88**, 1051 (2014).
22. T.N. Koltunowicz, P. Zukowski, O. Boiko, A. Saad, J.A. Fedotova, A.K. Fedotov, A.V. Larkin, J. Kasiuk, J. Electron. Mater. **44**, 2260 (2015).
23. K. Funke, Prog. Solid St. Chem. **22**, 111 (1993).
24. A.K. Jonscher, *Dielectric Relaxation in Solids* (Chelsea Dielectrics Press, London, 1983).
25. S. Sumi, P.P. Rao, M. Deepa, P. Koshy, J. Appl. Phys. **108**, 063718 (2010).
26. M. Pollak, Philos. Mag. B **65**, 657 (1992).
27. A.G. Zabrodskii, A.G. Andreev, S.V. Egorov, Phys. Status Solidi B **205**, 61 (1998).
28. A.G. Zabrodskii, Philos. Mag. B **81**, 1131 (2001).
29. A.L. Efros, B.I. Shklovskii, J. Phys. C **8**, L49 (1975).
30. S.R. Elliott, Philos. Mag. **36**, 1291 (1977).